Published in final edited form as:
Heart Rhythm. 2007 August ; 4(8): 1072–1080.

NOVEL MUTATION IN THE SCN5A GENE ASSOCIATED WITH ARRHYTHMIC STORM DEVELOPING DURING ACUTE MYOCARDIAL INFARCTION

Dan Hu, MD, PhD[1,2], **Sami Viskin, MD**[3], **Antonio Oliva, MD, PhD**[1,4], **Tabitha Carrier, BS**[1], **Jonathan M. Cordeiro, PhD**[1], **Hector Barajas-Martinez, PhD**[1,5], **Yuesheng Wu, MS**[1], **Elena Burashnikov, MS**[1], **Serge Sicouri, MD**[1], **Ramon Brugada, MD**[1], **Rafael Rosso, MD**[4], **Alejandra Guerchicoff, PhD**[1], **Guido D. Pollevick, PhD**[1], and **Charles Antzelevitch, PhD, FHRS**[1]

1*Masonic Medical Research Laboratory, Utica, New York, USA*

2*Department of Cardiology, Renmin Hospital of Wuhan University, Wuhan, Hubei, China*

3*Department of Cardiology, Tel-Aviv Sourasky Medical Center, and Sackler School of Medicine, Tel-Aviv University, Israel*

4*Institute of Forensic Medicine, Catholic University, Rome, Italy*

5*South University Center (CUSUR) and Human Genetics Programs of the University of Guadalajara (CIBO-CUCS), Cd. Guzman, Jalisco, México*

Abstract

Background—Ventricular tachycardia and fibrillation (VT/VF) complicating Brugada syndrome, a genetic disorder linked to SCN5A mutations, and VF complicating acute myocardial infarction (AMI) have both been linked to phase 2 reentry.

Objective—Because of these mechanistic similarities in arrhythmogenesis, we examined the contribution of SCN5A mutations to VT/VF complicating AMI.

Methods—Nineteen consecutive patients developing VF during AMI were enrolled. Wild-type (WT) and mutant SCN5A genes were co-expressed with SCN1B in TSA201 cells and studied using whole-cell patch-clamp techniques.

Results—One missense mutation (G400A) in SCN5A was detected in a conserved region among the cohort of 19 patients. A H558R polymorphism was detected on the same allele. Unlike the other 18 patients who each developed 1-2 VF episodes during acute MI, the mutation carrier developed six episodes of VT/VF within the first 12 hours. All VT/VF episodes were associated with ST segment changes and were initiated by short-coupled extrasystoles. A flecainide and adenosine challenge performed to unmask Brugada and long QT syndromes were both negative. Peak G400A and G400A +H558R current were 70.7% and 88.4% less than WT current at -35mV ($P \leq 0.001$). G400A current decay was accelerated and steady-state inactivation was shifted -6.39 mV ($V_{1/2}$=-98.9±0.1 mV vs. -92.5±0.1 mV, $P \leq 0.001$). No mutations were detected in KCNH2, KCNQ1, KCNE1 or KCNE2 in the G400A patient.

Address for editorial correspondence and reprint requests: Charles Antzelevitch, PhD, FACC, FAHA, FHRS, Gordon K. Moe Scholar, Masonic Medical Research Laboratory, 2150 Bleecker Street, Utica, New York, U.S.A. 13501-1787, Phone: (315) 735-2217, FAX: (315) 735-5648, E-mail: ca@mmrl.edu

There are no conflicts of interest or financial disclosures.

Conclusions—We describe the first sodium channel mutation to be associated with the development of an arrhythmic storm during acute ischemia. These findings suggest that a loss of function in SCN5A may predispose to ischemia-induced arrhythmic storm.

Keywords

Ventricular tachycardia; fibrillation; arrhythmia; ischemia; sudden cardiac death

INTRODUCTION

Each year, nearly 1 million individuals in the United States suffer an acute myocardial infarction (AMI). Approximately 20% to 25% experience sudden cardiac death soon after due to the development of ventricular tachycardia and fibrillation (VT/VF).[1] Although identification of patients at risk for primary VF during AMI remains rather poor, recent reports have highlighted the importance of family history, pointing to the possibility of a genetic predisposition.[2]

The SCN5A gene encodes for the α-subunit of the human cardiac voltage-gated sodium channel $hNa_v1.5$. The protein product of this gene expresses in the membrane with one or more β-subunits,[3] to initiate the action potential in virtually all cardiac cells except sinoatrial and atrioventricular nodal cells. The sodium channel current (I_{Na}) generated by the transmembrane channel formed by these subunits activates and inactivates within a few milliseconds. It also produces a very small persistent inward sodium current (late I_{Na}) that helps to maintain the action potential plateau. A loss and gain of function of the peak and late current have been linked to the development of reentrant and triggered arrhythmias, respectively.

SCN5A mutations thus far described have been linked to sudden cardiac death associated with a number of inherited arrhythmic syndromes, including the LQT3 form of the long QT syndrome, conduction disease, atrial standstill and Brugada Syndrome (BS).[4, 5] However, their association with acquired forms of VF is not well defined. Since mechanistic similarities exist between the VT/VF caused by Brugada syndrome and that caused by VT/VF associated with myocardial ischemia (both are linked to phase 2 reentry), we hypothesized that SCN5A mutations similar to those linked to Brugada syndrome, may predispose to the development of VT/VF during AMI.

The purpose of this study was to examine the contribution of SCN5A mutations to arrhythmogenesis in a cohort of patients who developed one or more episodes of VT/VF during acute myocardial infarction (AMI).

METHODS

Clinical Analysis

Nineteen consecutive patients admitted with AMI who developed ventricular fibrillation (VF) immediately prior to, or shortly after arrival to the intensive care unit, were studied. All patients had obvious ST segment elevation and elevation of cardiac enzymes diagnostic of AMI.

Mutation Analysis of SCN5A

Genetic analysis was performed to examine the contribution of SCN5A mutations to arrhythmogenesis during AMI following written informed consent and approval from the regional Institutional Review Board. Genomic DNA was isolated from peripheral blood leukocytes using a commercial kit (Gentra System, Puregene). The exons of SCN5A gene were amplified and analyzed by direct sequencing. Polymerase chain reaction (PCR) products were purified with a commercial reagent (ExoSAP-IT, USB) and were directly sequenced from both

directions using ABI PRISM 3100-Avant Automatic DNA sequencer. Genomic DNA from 182 ethnically-matched (Caucasian) healthy subjects, including 80 Ashkenazi Jews, was used as controls. We performed two independent PCRs to validate the nucleotide change. To assess whether G400A and H558R variations reside on the same allele, PCR experiments using the following primer sets: SCN5A exon 10 sense CTAGACTAGGTGACTTGGAAATG and SCN5A exon 12a antisense GCTGTTCTTTTTGCCATGGAGG were performed, followed by cloning of the PCR products into a Topo TA vector (Invitrogen, Carlsbad, CA). Nineteen clones were directly sequenced in both directions using ABI PRISM 3100-Avant Automatic DNA sequencer (Applied Biosystems, Foster City, CA).

Mutagenesis and Transfection of the TSA201 Cell Line

Mutant SCN5A channel was prepared using the Gene Tailor Site-Directed Mutagenesis System (Invitrogen, Carlsbad, CA) on full length wild type SCN5A cDNA (hH1a) cloned into pcDNA3.1+ (Invitrogen). The mutated SCN5A was sequenced to ensure the presence of mutation without spurious substitutions. Sodium channels were expressed in modified human embryonic kidney cell line TSA201 as previously described.[6] Briefly, TSA201 cells were co-transfected with 12 μg of SCN5A (WT, G400A or G400A/H558R) and 4 μg of SCN1B (β1 subunit) using the calcium phosphate precipitation method. In addition CD_8 cDNA (4 μg) was co-transfected as reporter gene to visually identify transfected cells using Dynabeads (M-450 CD8 Dynal). The cells were grown on polylysine coated 35 mm culture dishes and placed in a temperature-controlled chamber at 37°C for 24 to 72 hours and then studied at room temperature.

Patch Clamp Method

Membrane currents were measured using whole-cell patch-clamp techniques in transfected TSA201 cells. All recordings were obtained at room temperature (22°C) using an Axopatch 200B amplifier equipped with a CV-201A head stage (Axon Instruments, San Francisco, CA). Measurements were started 10 minutes after obtaining the whole-cell configuration to allow the current to stabilize. The holding potential was maintained at -120 mV. Macroscopic whole cell Na^+ current was recorded by using bath solution perfusion containing (in mmol/L) 140 NaCl, 5 KCl, 1.8 $CaCl_2$, 1 $MgCl_2$, 2.8 Na Acetate, 10 HEPES, 10 Glucose (pH 7.3 with NaOH). Tetraethylammonium Chloride (5 mmol/ L) was added to the buffer to block TEA-sensitive native currents. Patch pipettes were fabricated from borosilicate glass capillaries (1.5 mm O.D., Fisher Scientific, Pittsburgh, PA). They were pulled using a gravity puller (Model PP-89, Narishige Corp, Japan) to obtain a resistances between 0.8 - 2.8 MΩ when filled with a solution containing (in mmol/L) 5 NaCl, 5 KCl, 130 CsF, 1.0 $MgCl_2$, 5 EGTA and 10 HEPES (pH 7.2 with CsOH). Currents were filtered with a four pole Bessel filter at 5 kHz and digitized at 50 kHz. Series resistance was electronically compensated at 70-85%.

The parameters for voltage dependence of activation were estimated from the current voltage relation based on the equation: $I = G_{max}\cdot(V-V_{rev})/(1+\exp(-(V\ V_{1/2})/k)$, where I is the peak current amplitude, G_{max} the maximum conductance, V test potential, V_{rev} the reversal potential, $V_{1/2}$ the midpoint of activation, and k the slope factor. Steady-state availability was fitted to the Boltzmann equation, $I/\ I_{max}= 1/(1+\exp((V-V_{1/2})/k))$ to determine the membrane potential for half-maximal inactivation $V_{1/2}$ and the slope factor k. Recovery from inactivation was analyzed by fitting data to a double exponential function: $I_{(t)}/I_{max}= A_f\cdot(1-\exp(-t/\tau_f))+A_s\cdot(1-\exp(-t/\tau_s))$, where A_f and A_s are the fractions of fast and slow inactivating components, respectively, and τ_f and τ_s are their time constants.

All data acquisition and analysis were performed using pCLAMP V9.2 (Axon Instruments, Foster City, CA), EXCEL (Microsoft) and ORIGIN 7.0 (Microcal Software, Northampton, MA).

Statistical Analysis

Data are expressed as mean ± SEM. Two-tailed Student's t-test and ANOVA coupled with a Student-Newman-Keuls test were used for statistical analysis, as appropriate (SigmaStat, Jandel Scientific Software). Differences were considered to be statistically significant at a value of $P<0.05$.

RESULTS

Clinical Observations

Nineteen patients (18 males), aged 57 ± 10 years, admitted with anterior (9 patients) and inferior (10 patients) myocardial infarction (MI) were studied (Table 1). All patients had preserved left ventricular ejection fraction, reflecting the fact that (for all except 1 patient), this was the first myocardial infarction. All patients underwent cardiac catheterization and significant coronary artery stenosis was documented in all but 2 patients. One of these 2 patients had irregularities with a suspected thrombus in the culprit artery while the other patient had repeated documented spontaneous coronary artery spasm before and during catheterization (Table 1).

One patient (MMRL23) presented with an arrhythmic storm, displaying 6 episodes of polymorphic VT and VF within the first 12 hours (Figure 1A to 1F). This 70-year old male with a history of coronary disease was hospitalized because of angina exacerbation. Cardiac catheterization revealed good left ventricular function with moderate aortic regurgitation as well as an 80% restenosis within a stent previously implanted in the proximal left anterior descending (LAD) coronary artery. The patient underwent aortic valve replacement and bypass surgery [left internal mammary artery (LIMA) to LAD]. That hospitalization course was uneventful and the patient was discharged after 5 days. However, he returned 2 days later with an evolving anterior myocardial infarction (Figure 1A). Shortly thereafter, he developed ventricular fibrillation (VF) (Figure 1B). Several episodes of non-sustained polymorphic VT (Figure 1D) and VF requiring defibrillation (Figure 1B and 1F) occurred during the first day of hospitalization. Review of the ECG revealed marked ST segment depression preceding all polymorphic VT/VF episodes, which were triggered by a short-coupled extrasystole (Figure 1B, 1D, 1E). This sequence of events strongly suggested that the VT/VF episodes were related to acute myocardial ischemia and the patient underwent cardiac catheterization again. This revealed that the known in-stent stenosis had progressed to total occlusion of the proximal LAD. Competitive flow from the LIMA reached the distal end of the occluded stent. However, haziness at the LIMA to LAD anastomosis suggested the possibility of intermittent occlusion with spontaneous reperfusion had caused the infarction. Because left ventricular function was preserved and the LIMA to LAD graft was now patent, the patient was treated conservatively.

The patient with the arrhythmic storm was the only one in which a SCN5A mutation was uncovered. The mutation carrier had no history of previous syncope or a history of familial sudden death. Moreover, he did not display ST segment elevation suggestive of Brugada syndrome at any time prior to the AMI. Finally, provocative tests with flecainide[7] and adenosine,[8] performed to exclude subclinical forms of Brugada syndrome and long QT syndrome, were both negative.

Molecular Genetics

PCR-based sequencing of all exons and exon-intron boundaries revealed H558R polymorphism (a histidine to arginine substitution at codon 558) between domain I and domain II in 5 of the 19 patients, and R34C polymorphism (an arginine to cysteine substitution at codon 34) in the C-terminal of SCN5A in one patient. These heterozygous polymorphisms are common in the population, appearing with a frequency of 20% and 4%, respectively.[9]

All but one patient tested negative for a SCN5A mutation. MMRL23, the only patient with the arrhythmic storm, presented with a novel missense mutation combined with H558R polymorphism in the same allele of the SCN5A gene (Figure 2B). PCR-based sequencing analysis revealed a double peak in the sequence of exon 10 of the SCN5A gene (Figure 2A) showing a G-to-C transversion at nucleotide 1199 predicting an amino acid substitution of Gly for Ala at codon 400 (designated G400A). This nucleotide change was not observed in 364 reference alleles, suggesting that this variation represents a disease-related mutation. Gly-400 is located in the S6 transmembrane segment of domain I of SCN5A (Figure 2B) and is highly conserved among the members of the voltage-gated sodium channel α-subunit family and through evolution (Figure 2C).

Because the QT interval was slightly prolonged during the early phase of recovery from myocardial infarction (MI), we screened this patient for 4 of the common long QT genes KCNH2, KCNQ1, KCNE1 and KCNE2. No mutations were detected in any of these genes. A G38S heterozygous polymorphism was detected in KCNE1. This is a common polymorphism with a heterozygous frequency of 36.1 to 44.9% (Table 2).[10]

Electrophysiological Characteristics of the WT, G400A and G400A+H558R

The G400A, G400A+H558R mutant and the wild-type (WT) sodium channel were expressed in TSA201 cells to assess the effects of the mutation on sodium channel function (Figure 3A) shows macroscopic currents recorded from WT, G400A and G400A+H558R channels. The current-voltage (I-V) relationship suggests that maximum peak inward current occurs at a potential of -35 mV for all channel types, but the current amplitude of G400A was much smaller than that of WT. The presence of the H558R polymorphism in the same gene resulted in a further decrease in peak I_{Na} (Figure 3B). There was a significant difference in peak current amplitude from -50 mV to -15 mV between G400A and WT, from -50 mV to +5 mV between G400A+H558R and WT, and from -40 mV to -15 mV between G400A+H558R and G400A (Figure 3B). Peak G400A and G400A+H558R current at -35 mV decreased 70.7% and 88.4% relative to WT, respectively ($P \leq 0.001$ and $P \leq 0.001$). The voltage dependence of steady-state activation of G400A was shifted +1.32 mV ($P \leq 0.001$), but the slope factor was not significantly altered (Figure 3C).

Steady-state inactivation was measured in WT and G400A channels by varying the conditioning pulse between -140 mV and -60 mV to inactivate the channels followed by a test pulse to -20 mV (Figure 4A). The mid-inactivation voltage of steady-state inactivation in G400A was shifted by 6.39 mV in the hyperpolarizing direction and the slope factor was significantly larger (Figure 4B). As a consequence there was a smaller overlap in the relationship between channel inactivation and activation (window current). Of note, G400A +H558R current was too small to evaluate steady-state activation and inactivation characteristics.

Using a standard double paired-pulse protocol, the rate of recovery from inactivation was shown to be significantly slower for G400A channels when compared to WT (Figure 5A and Figure 5B).

G400A channels were also evaluated for persistent inward sodium current. Na^+ currents of WT and G400A were recorded at -20mV, from a holding potential of -120mV in the absence and presence of 25 μmol/L TTX (Figure 6A). Neither WT nor G400A showed a substantial persistent inward TTX-sensitive late current at the end of a 300-ms depolarization. Late I_{Na} recorded from the G400A channel was significantly smaller than in WT ($P < 0.05$), although the ratio of late I_{Na} to peak I_{Na} was not statistically different between G400A and WT channels (Figure 6B).

DISCUSSION

Experimental studies indicate that a rebalancing of currents active during the early phases of the action potential can give rise to prominent ST segment changes and create the substrate for the development of reentrant arrhythmias under ischemic conditions as well as in inherited sudden death syndromes such as the Brugada syndrome.[11-14] It has been suggested that the two may be additive or synergistic.[15] Recent clinical studies have provided support for this hypothesis demonstrating a synergism between ST segment elevation and arrhythmogenesis in patients with the Brugada syndrome when an ischemic insult is superimposed.[16]

In the Brugada syndrome, sodium channel blockers are known to unmask the syndrome regardless of genotype and loss-of-function SCN5A mutations have been identified as causative in 20% of cases.[17-19] In the present study, we provide evidence in support of the corollary hypothesis that SCN5A mutations can exacerbate arrhythmogenesis in the setting of AMI. Our findings suggest a genetic predisposition for acquired (i.e., ischemia related) VF in 1 out of 19 patients with AMI complicated by VF. A similar percentage of genetic anomalies predisposing to ventricular arrhythmias have been reported for other forms of “acquired arrhythmic syndromes”, such as drug-induced long QT syndrome.[20]

The patient carrying the SCN5A mutation was the only one who developed an arrhythmic storm during AMI in our small series. The fact that this patient developed his first VF only at 70 years of age and only in the setting of AMI supports the notion that the SCN5A mutation in this patient was a predisposing factor for the acquired arrhythmic syndrome. Further support for this hypothesis derives from the absence of a coved type ST segment elevation typical of Brugada syndrome, either spontaneously or during a flecainide challenge test.

The G400A missense mutation in SCN5A was found to create several defects in the function of the sodium channel, including a markedly reduced current density, impaired recovery from inactivation, and shift in the voltage dependence of inactivation to hyperpolarized potentials. The functional consequence of these changes is likely to be a reduced Na^+ current during the upstroke of the action potential.

Our G400A carrier had a common polymorphism (H558R) on the same allele, which in the case of some mutations, such as M1766L, has been shown to alter the expressed phenotype. Co-expression of H558R with the M1766L mutation has been shown to correct the trafficking defect observed with the mutation alone[21] or to mitigate the loss of function produced by T512I.[22] Another report has also demonstrated that H558R polymorphism rescued defective intracellular trafficking of R282H and reconstituted I_{Na} current in heterologous expression system.[23] On the other hand, the R558-encoding allele yields a sodium channel with reduced function when expressed in the context of the Q1077-containing transcript, which is the minor alternatively spliced transcript, accounting for approximately one third of SCN5A transcripts.[24, 25] Our study is the first to demonstrate an effect of H558R to further accentuate the effect of a loss of function mutation.

Although our understanding of the role of loss and gain of function of I_{Na} in inherited syndromes such as Brugada and long QT syndromes has crystallized in recent years, less is known about the mechanisms linking impaired sodium channel gating to ECG and arrhythmic manifestations in acquired VF.

A reduced level of I_{Na}, secondary to SCN5A mutations or otherwise, can facilitate the development of arrhythmogenesis by reducing excitability, slowing conduction and thus facilitating reentry in the setting of AMI. However, the absence of QRS widening during AMI and immediately preceding VF episodes in our patient, favor a different mechanism. Another possibility is that the reduced sodium channel current leaves transient outward current (I_{to})

unopposed. This outward shift in current allows phase 1 to proceed to more negative potentials. All-or-none repolarization leading to loss of the action potential dome generally occurs when phase 1 reaches potentials of approximately -30 mV. These effects of loss of function of I_{Na}, which have been shown to be responsible for promoting arrhythmogenesis in the Brugada syndrome, are likely responsible for facilitating arrhythmogenesis during AMI. Reduced peak I_{Na} can selectively hasten epicardial repolarization, thus creating both the substrate and trigger for reentry, accounting for the arrhythmic storm and observed ischemia-related change in ECG. Of note, VT/VF episodes in our mutant carrier were all precipitated by closely coupled extrasystoles (<390 msec), consistent with a phase 2 reentrant mechanism.

Despite similar changes in resting membrane potential, ischemia induces a greater depression of the action potentials of ventricular epicardial versus endocardial tissues.[26, 27] Studies performed in isolated canine ventricular epicardial and endocardial tissues have demonstrated that intrinsic cellular electrophysiological differences form the basis for the differential sensitivity to ischemic conditions.[11, 12, 28-30] The presence of a prominent transient outward current (I_{to})-mediated spike and dome morphology (notch) in epicardium[31] was shown to be, in large part, responsible for the differential response. In isolated endocardial and epicardial preparations, superfusion with a simulated “ischemic” Tyrode’s solution induces an all-or-none repolarization at the end of phase 1 leading to loss of the epicardial action potential dome and marked abbreviation of the action potential.[11]

The presence of a large epicardial I_{to} is essential for all-or-none repolarization. It is for this reason that, loss of the epicardial action potential dome observed under ischemic conditions and conditions mimicking “components” of ischemia (pinacidil-induced $I_{K(ATP)}$ activation,[28] elevated extracellular calcium combined with rapid pacing,[29] occurs preferentially in right ventricular (RV) epicardial tissues, where I_{to} is most prominent.[32]

The effect of coronary occlusion to give rise to a differential loss of the action potential dome in epicardium, resulting in the development of ST segment elevation and arrhythmogenesis has recently been demonstrated in isolated coronary-perfused ventricular wedge preparations.[14, 33] Heterogeneous loss of the action potential dome during ischemia has been shown to give rise to transmural dispersion of repolarization as well as phase 2 reentry, thus precipitating reentry in the form of VT/VF.[12, 14, 33]

Because SCN5A mutations are known to contribute to arrhythmogenesis in a variety of inherited diseases, including Long QT and Brugada syndromes, we made an effort to ascertain whether our G400A carrier has a subclinical form of these syndromes. The mutation carrier tested negative to a sodium block challenge involving flecainide designed to unmask the Brugada syndrome, as well as to adenosine, a provocative test designed to unmask the long QT syndrome. The common long QT genes were screened and found to contain no mutations.

Study Limitations

Our results suggest that a subclinical mutation in SCN5A resulting in a loss of function may predispose to life-threatening arrhythmias during acute ischemia. Our data support the hypothesis that the loss of function mutation in SCN5A facilitates arrhythmogenesis attending acute MI, but because of their limited nature are no more than hypothesis-forming. A more extensive study is clearly needed to test this hypothesis.

ACKNOWLEDGEMENTS

We are grateful to Robert Goodrow Jr., Judy Hefferon, Ryan Pfeiffer and Jeremy Stewart for expert technical assistance.

Supported by grants HL47678 (CA) and HL66169 (RB) from NHLBI, and grants from the American Heart Association (RB), National Heart Foundation, a program of the American Health Assistance Foundation (JMC), and NYS and Florida Grand Lodges, F. & A.M.

Abbreviations

AMI, acute myocardial infarction; BS, Brugada syndrome; I_{Na}, sodium channel current; I_{to}, transient outward current; LAD, left anterior descending; LIMA, left internal mammary artery; LQT3, form of the long QT syndrome; MI, myocardial infarction; PCR, polymerase chain reaction; RV, right ventricular; VF, ventricular fibrillation; VT/VF, Ventricular tachycardia and fibrillation; WT, Wild-type.

References

1. Solomon SD, Zelenkofske S, McMurray JJ, Finn PV, Velazquez E, Ertl G, Harsanyi A, Rouleau JL, Maggioni A, Kober L, White H, Van de WF, Pieper K, Califf RM, Pfeffer MA. Sudden death in patients with myocardial infarction and left ventricular dysfunction, heart failure, or both. N Engl J Med 2005;352:2581–8. [PubMed: 15972864]
2. Dekker LR, Bezzina CR, Henriques JP, Tanck MW, Koch KT, Alings MW, Arnold AE, de Boer MJ, Gorgels AP, Michels HR, Verkerk A, Verheugt FW, Zijlstra F, Wilde AA. Familial sudden death is an important risk factor for primary ventricular fibrillation: a case-control study in acute myocardial infarction patients. Circulation 2006;114:1140–5. [PubMed: 16940195]
3. Catterall WA. Cellular and molecular biology of voltage-gated sodium channels. Physiol Rev 1992;72:S15–S48. [PubMed: 1332090]
4. Roden DM. Human genomics and its impact on arrhythmias. Trends Cardiovasc Med 2004;14:112–6. [PubMed: 15121159]
5. Antzelevitch C. Molecular genetics of arrhythmias and cardiovascular conditions associated with arrhythmias. Heart Rhythm 2004;1:42C–56C.
6. Dumaine R, Towbin JA, Brugada P, Vatta M, Nesterenko DV, Nesterenko VV, Brugada J, Brugada R, Antzelevitch C. Ionic mechanisms responsible for the electrocardiographic phenotype of the Brugada syndrome are temperature dependent. Circ Res 1999;85:803–9. [PubMed: 10532948]
7. Brugada R. Use of intravenous antiarrhythmics to identify concealed Brugada syndrome. Curr Control Trials Cardiovasc Med 2000;1:45–7. [PubMed: 11714408]
8. Viskin S, Rosso R, Rogowski O, Belhassen B, Levitas A, Wagshal A, Katz A, Fourey D, Zeltser D, Oliva A, Pollevick GD, Antzelevitch C, Rozovski U. Provocation of sudden heart rate oscillation with adenosine exposes abnormal QT responses in patients with long QT syndrome: a bedside test for diagnosing long QT syndrome. Eur Heart J 2006;27:469–75. [PubMed: 16105845]
9. Kaab S, Schulze-Bahr E. Susceptibility genes and modifiers for cardiac arrhythmias. Cardiovasc Res 2005;67:397–413. [PubMed: 15949790]
10. Ackerman MJ, Tester DJ, Jones GS, Will ML, Burrow CR, Curran ME. Ethnic differences in cardiac potassium channel variants: implications for genetic susceptibility to sudden cardiac death and genetic testing for congenital long QT syndrome. Mayo Clin Proc 2003;78:1479–87. [PubMed: 14661677]
11. Lukas A, Antzelevitch C. Differences in the electrophysiological response of canine ventricular epicardium and endocardium to ischemia: Role of the transient outward current. Circulation 1993;88:2903–15. [PubMed: 8252704]
12. Lukas A, Antzelevitch C. Phase 2 reentry as a mechanism of initiation of circus movement reentry in canine epicardium exposed to simulated ischemia. Cardiovasc Res 1996;32:593–603. [PubMed: 8881520]
13. Yan GX, Antzelevitch C. Cellular basis for the Brugada Syndrome and other mechanisms of arrhythmogenesis associated with ST segment elevation. Circulation 1999;100:1660–6. [PubMed: 10517739]
14. Yan GX, Joshi A, Guo D, Hlaing T, Martin J, Xu X, Kowey PR. Phase 2 Reentry as a Trigger to Initiate Ventricular Fibrillation During Early Acute Myocardial Ischemia. Circulation 2004;110:1036–41. [PubMed: 15302777]

15. Antzelevitch C, Brugada P, Brugada J, Brugada R, Nademanee K, Towbin JA. Clinical Approaches to Tachyarrhythmias. The Brugada Syndrome 1999:1–99.
16. Noda T, Shimizu W, Taguchi A, Satomi K, Suyama K, Kurita T, Aihara N, Kamakura S. ST-segment elevation and ventricular fibrillation without coronary spasm by intracoronary injection of acetylcholine and/or ergonovine maleate in patients with Brugada syndrome. J Am Coll Cardiol 2002;40:1841–7. [PubMed: 12446069]
17. Chen Q, Kirsch GE, Zhang D, Brugada R, Brugada J, Brugada P, Potenza D, Moya A, Borggrefe M, Breithardt G, Ortiz-Lopez R, Wang Z, Antzelevitch C, O'Brien RE, Schultze-Bahr E, Keating MT, Towbin JA, Wang Q. Genetic basis and molecular mechanisms for idiopathic ventricular fibrillation. Nature 1998;392:293–6. [PubMed: 9521325]
18. Schulze-Bahr E, Eckardt L, Breithardt G, Seidl K, Wichter T, Wolpert C, Borggrefe M, Haverkamp W. Sodium channel gene (SCN5A) mutations in 44 index patients with Brugada syndrome: different incidences in familial and sporadic disease. Hum Mutat 2003;21:651–2. [PubMed: 14961552]
19. Smits JP, Eckardt L, Probst V, Bezzina CR, Schott JJ, Remme CA, Haverkamp W, Breithardt G, Escande D, Schulze-Bahr E, LeMarec H, Wilde AA. Genotype-phenotype relationship in Brugada syndrome: electrocardiographic features differentiate SCN5A-related patients from non-SCN5A-related patients. J Am Coll Cardiol 2002;40:350–6. [PubMed: 12106943]
20. Roden DM, Viswanathan PC. Genetics of acquired long QT syndrome. J Clin Invest 2005;115:2025–32. [PubMed: 16075043]
21. Ye B, Valdivia CR, Ackerman MJ, Makielski JC. A common human SCN5A polymorphism modifies expression of an arrhythmia causing mutation. Physiol Genomics 2003;12:187–93. [PubMed: 12454206]
22. Viswanathan PC, Benson DW, Balser JR. A common SCN5A polymorphism modulates the biophysical effects of an SCN5A mutation. J Clin Invest 2003;111:341–6. [PubMed: 12569159]
23. Poelzing S, Forleo C, Samodell M, Dudash L, Sorrentino S, Anaclerio M, Troccoli R, Iacoviello M, Romito R, Guida P, Chahine M, Pitzalis M, Deschenes I. SCN5A Polymorphism Restores Trafficking of a Brugada Syndrome Mutation on a Separate Gene. Circulation 2006;114:368–76. [PubMed: 16864729]
24. Makielski JC, Ye B, Valdivia CR, Pagel MD, Pu J, Tester DJ, Ackerman MJ. A ubiquitous splice variant and a common polymorphism affect heterologous expression of recombinant human SCN5A heart sodium channels. Circ Res 2003;93:821–8. [PubMed: 14500339]
25. Tan BH, Valdivia CR, Rok BA, Ye B, Ruwaldt KM, Tester DJ, Ackerman MJ, Makielski JC. Common human SCN5A polymorphisms have altered electrophysiology when expressed in Q1077 splice variants. Heart Rhythm 2005;2:741–7. [PubMed: 15992732]
26. Gilmour RF Jr. Zipes DP. Different electrophysiological responses of canine endocardium and epicardium to combined hyperkalemia, hypoxia, and acidosis. Circ Res 1980;46:814–25. [PubMed: 7379247]
27. Kimura S, Bassett AL, Kohya T, Kozlovskis PL, Myerburg RJ. Simultaneous recording of action potentials from endocardium and epicardium during ischemia in the isolated cat ventricle: Relation of temporal electrophysiologic heterogeneities to arrhythmias. Circulation 1986;74:401–9. [PubMed: 3731429]
28. Di Diego JM, Antzelevitch C. Pinacidil-induced electrical heterogeneity and extrasystolic activity in canine ventricular tissues. Does activation of ATP-regulated potassium current promote phase 2 reentry? Circulation 1993;88:1177–89. [PubMed: 7689041]
29. Di Diego JM, Antzelevitch C. High [Ca^{2+}]-induced electrical heterogeneity and extrasystolic activity in isolated canine ventricular epicardium. Phase 2 reentry. Circulation 1994;89:1839–50. [PubMed: 7511994]
30. Billman GE. Ro 40-5967, a novel calcium channel antagonist, protects against ventricular fibrillation. Eur J Pharm 1992;229:179–87.
31. Liu DW, Gintant GA, Antzelevitch C. Ionic bases for electrophysiological distinctions among epicardial, midmyocardial, and endocardial myocytes from the free wall of the canine left ventricle. Circ Res 1993;72:671–87. [PubMed: 8431990]
32. Di Diego JM, Sun ZQ, Antzelevitch C. I_{to} and action potential notch are smaller in left vs. right canine ventricular epicardium. Am J Physiol 1996;271:H548–H561. [PubMed: 8770096]

33. Di Diego JM, Antzelevitch C. Cellular basis for ST-segment changes observed during ischemia. J Electrocardiol 2003;36(Suppl):1–5. [PubMed: 14716579]

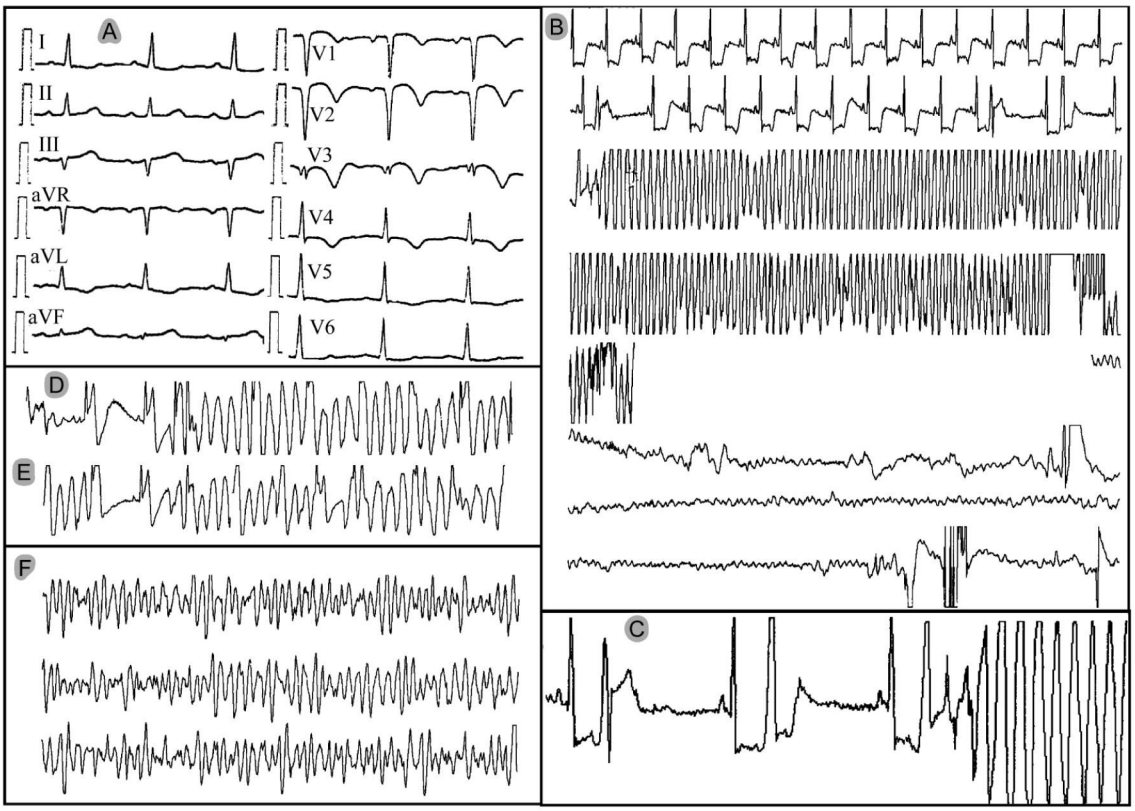

Figure 1.

Electrocardiograms of patient MMRL23 recorded during the first day of hospitalization. **A:** 12-lead electrocardiogram of evolving anterior myocardial infarction. **B to F:** single-lead monitor recordings. **B:** Episode of polymorphic VT deteriorating to VF. The transition from polymorphic VT to VF is missing because the monitor lead was disconnected during resuscitation. **C:** Onset of the VF episode shown in panel B. Note the accentuated ST depression and the short coupling interval (R-on-T phenomenon) of the ventricular ectopic beats, including the one initiating the polymorphic VT/VF. **D and E:** Additional episodes of non-sustained polymorphic VT starting with short-coupled extrasystoles. **F:** Additional VF episode that required electrical cardioversion (initiation not shown).

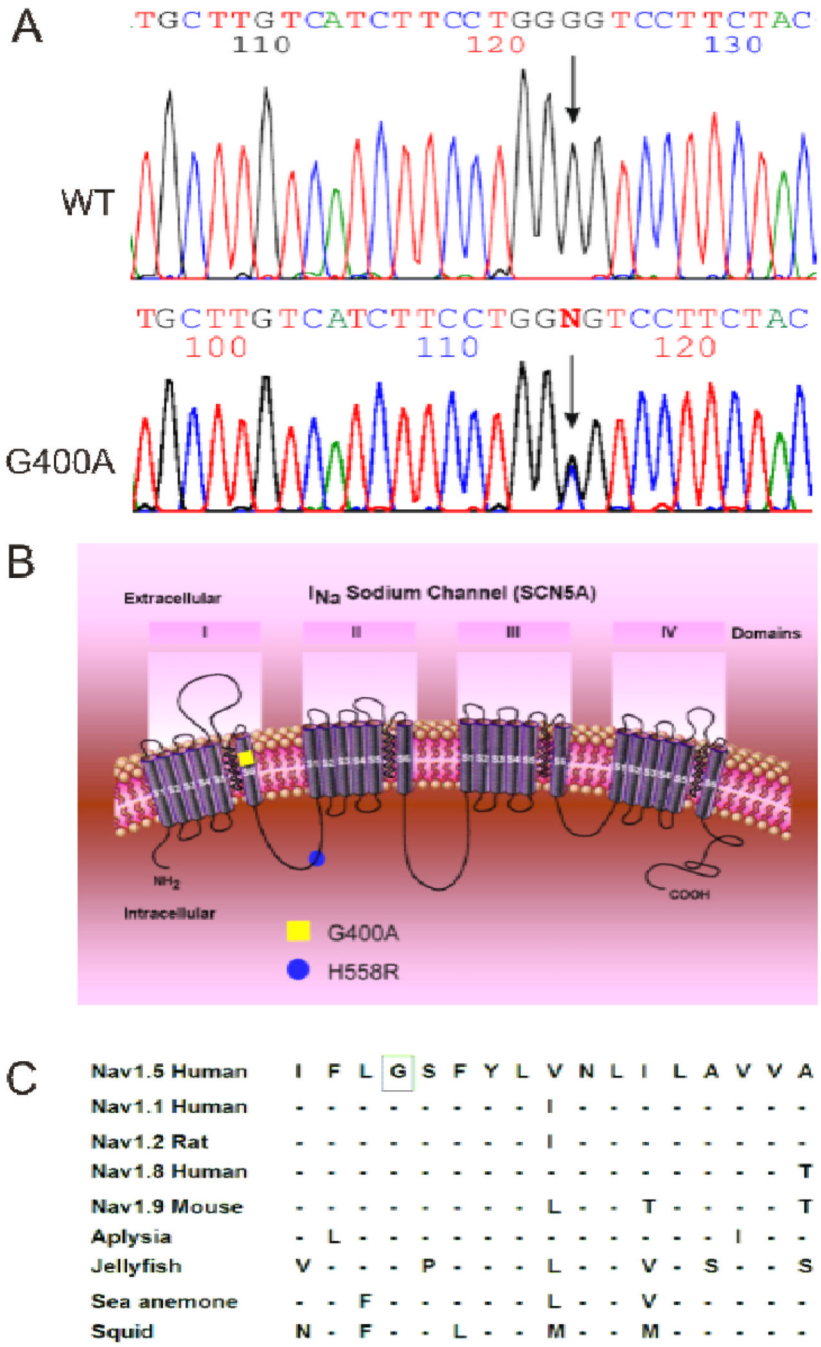

Figure 2.

Genetic analysis of patient MMRL23. **A:** PCR-based sequence of SCN5A exon 10 showing wild-type (WT) and G to C transversion at nucleotide 1199 (arrow) in patient MMRL23. The mutation predicts a substitution of Ala (GCG) for Gly (GGG) at position 400 (G400A). **B:** Location of the G400A mutation and H558R polymorphism are indicated using the conventional transmembrane topology model. **C:** Alignment of the voltage-gated sodium channel α-subunit family amino acid sequence, with related sequence shows that G400 is highly conserved among different sodium channels and different species. Dashes indicate identical residues to human SCN5A channel.

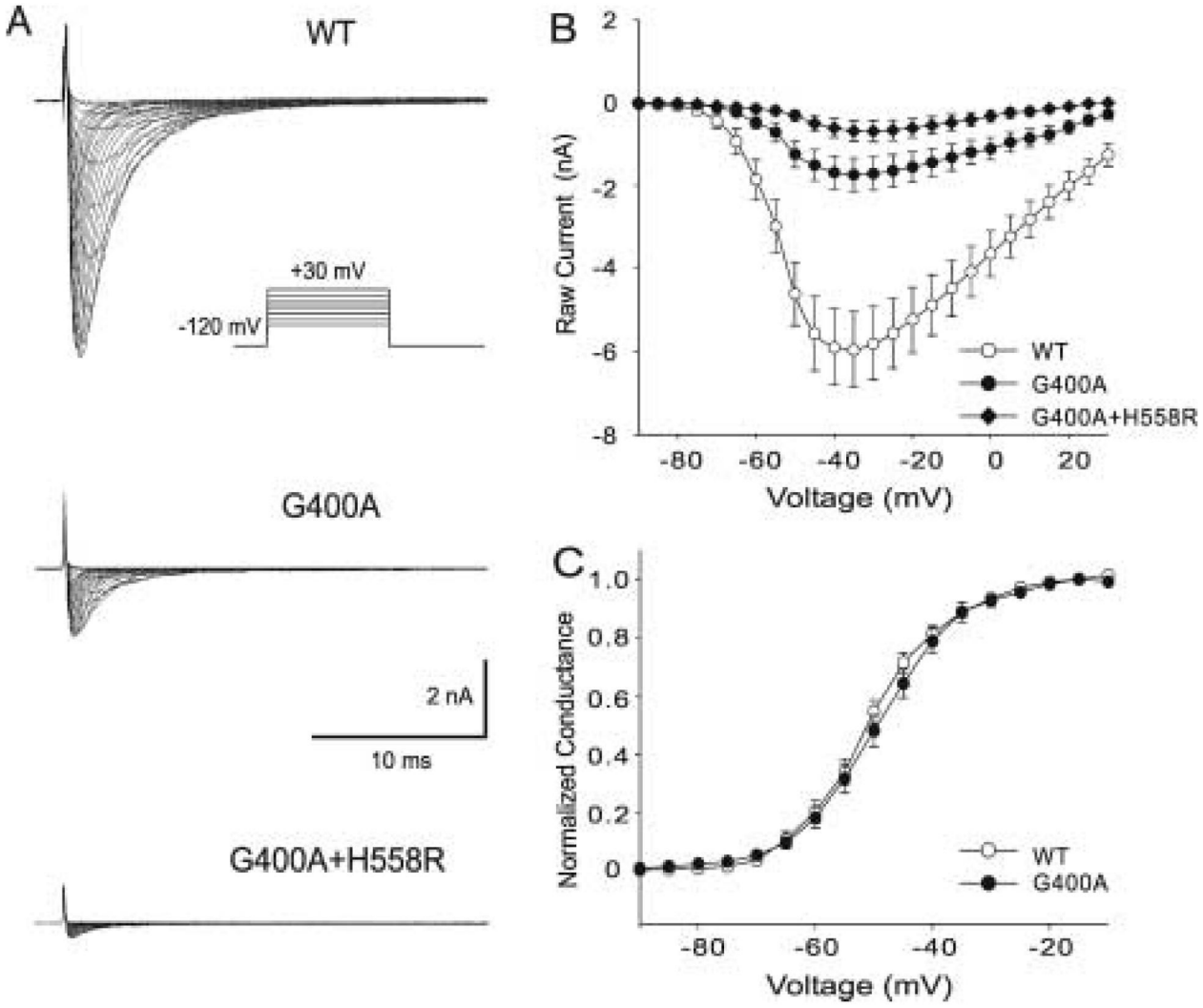

Figure 3.

Analysis of whole-cell current recorded from TSA201 cells expressing WT, G400A and G400A+H558R. **A:** Representative sodium current traces recording from WT and mutants. I_{Na} was elicited by depolarizing pulses ranging from -90 mV to +30 mV in 5 mV increments with a holding potential of -120 mV. The insets show the voltage-clamp protocols. **B:** Current-voltage relationship for WT (open circles, n = 33), G400A (filled circles, n = 14) and G400A +H558R (filled diamonds, n = 17). The current amplitude was significantly reduced for G400A when compared to WT at test potentials between -50 mV and -15 mV ($P < 0.001$ for -40 mV, -35 mV and -30 mV; $P < 0.005$ for -45 mV and -25 mV; $P < 0.05$ for -50 mV , -20 mV and -15 mV), G400A+H558R current was further reduced and shown to be significantly different from WT at test potentials between -50 mV and +5 mV ($P < 0.001$ form - 50 mV to -5 mV; $P < 0.005$ for 0 mV; $P < 0.05$ for 5 mV). G400A+H558R was also statistically different form G400A between -40 mV to -15 mV ($P < 0.05$). **C:** Voltage-dependent properties of activation for WT (open circles) and G400A (filled circles) sodium channels. Chord conductance was determined using the ration of current to the electromotive potential for the cells shown in Panel B one by one. Data were normalized and plotted against their test potential. For activation, $V_{1/2}$= -50.81 ± 0.18 mV and k = 6.88 ± 0.16 mV for WT, and $V_{1/2}$= -49.49 ± 0.10

mV and k = 7.27 ± 0.09 mV for G400A ($P \leq 0.001$ for difference in $V_{1/2}$; but no significant difference in k, P = 0.125).

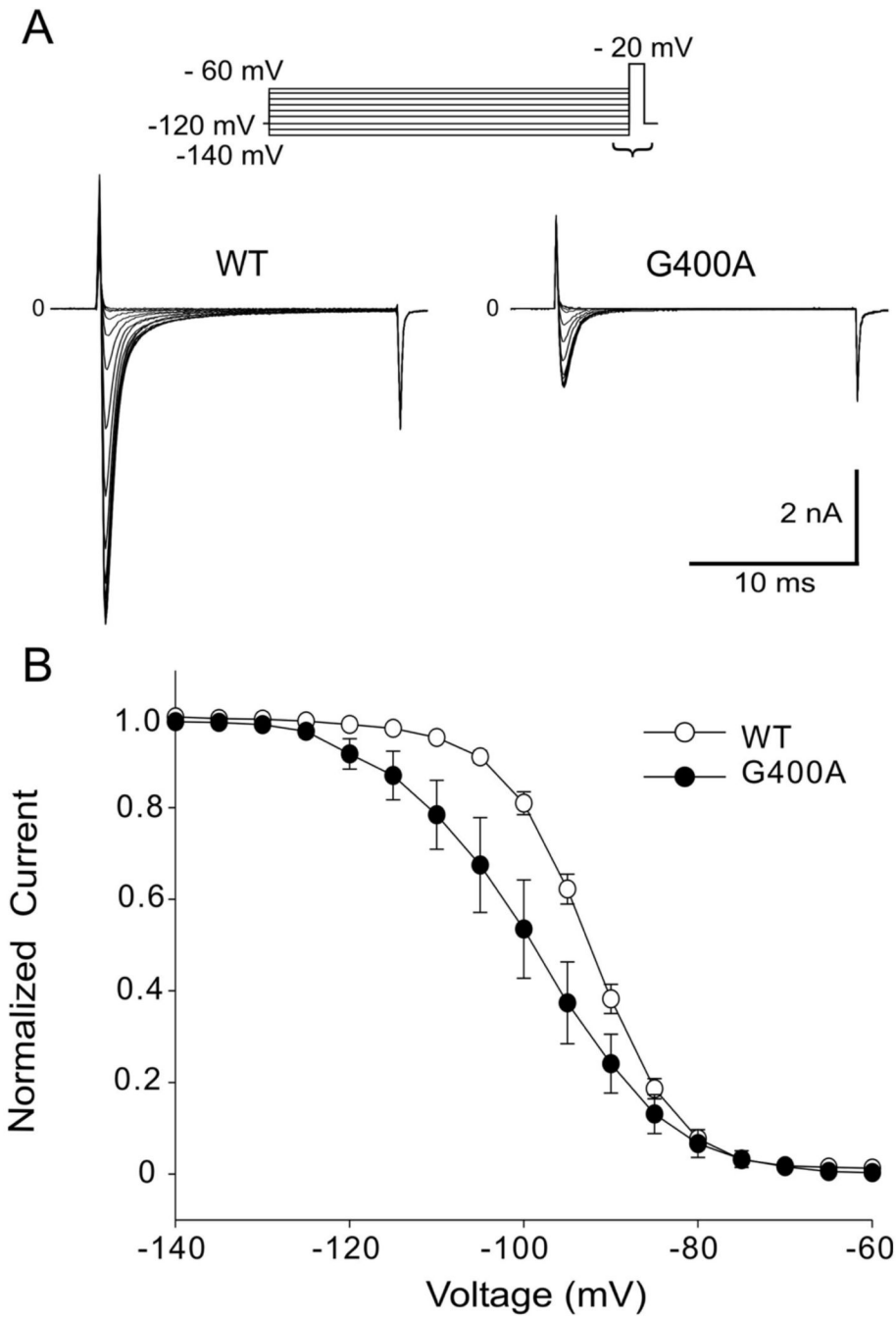

Figure 4.

Steady-State Inactivation in WT and G400A Channels. **A:** Representative Steady-state inactivation traces from both WT and mutant observer in response to the voltage clamp protocol on top of figure. **B:** Voltage-dependent properties of inactivation for WT (open circles, n =17) and G400A (filled circles, n = 9) sodium channels. Peak current was normalized to their respective maximum values and plotted against the conditioning potential. For inactivation, $V_{1/2}$= -92.53 ± 0.10 mV and k = 5.24 ± 0.09 mV for WT, and$V_{1/2}$= -98.92 ± 0.10 mV and k = 8.05 ± 0.09 mV for G400A ($P \leq 0.001$ for differences in $V_{1/2}$and k). Data were fitted by Boltzman function.

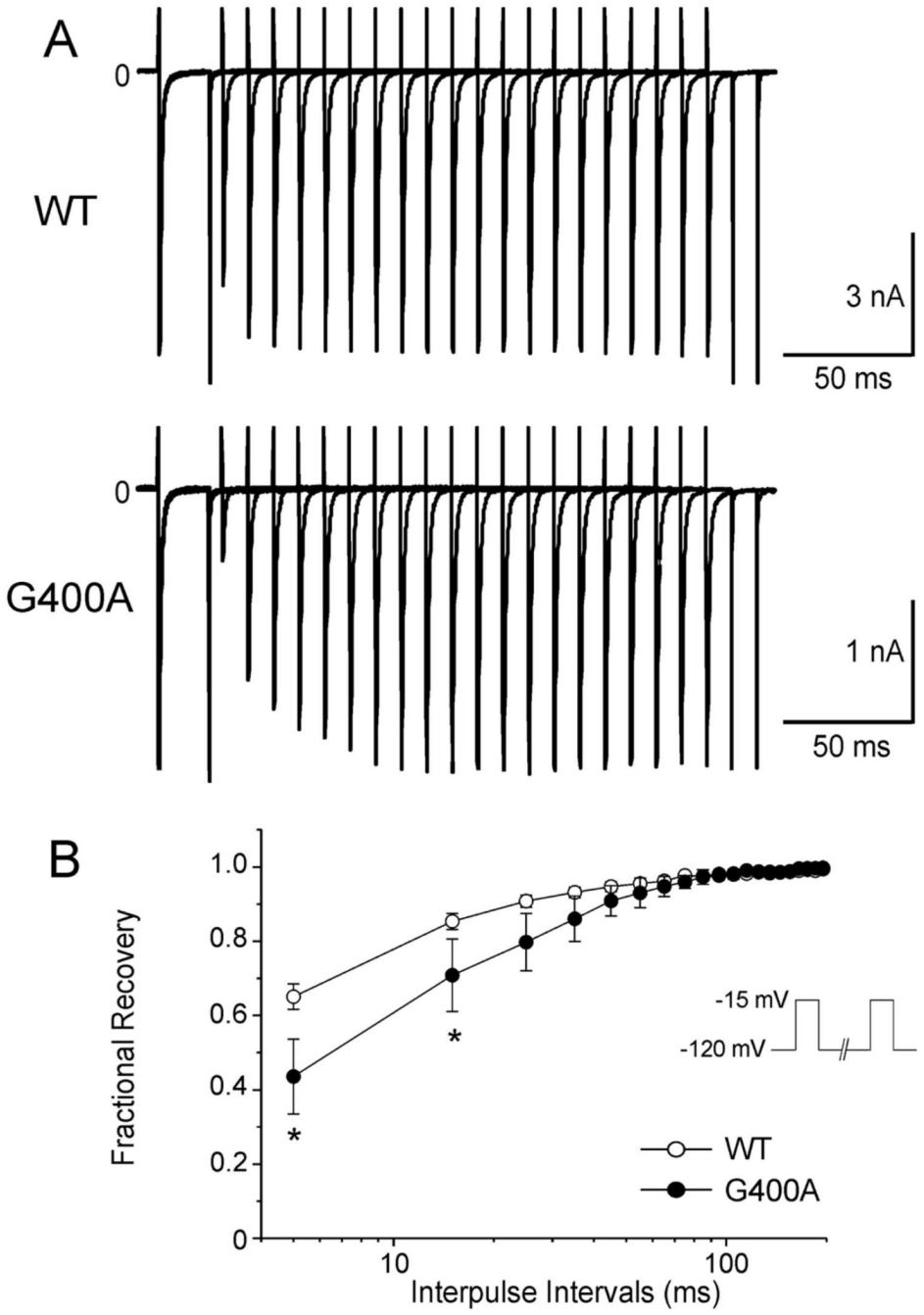

Figure 5.

Recovery from fast inactivation of WT and G400A mutant channels. **A:** Representative traces of recovery in WT and G400A were studied using the two-pulse protocol shown in the inset of panel B. **B:** Overlap in time constants of the recovery from fast inactivation. Peak current elicited during the second pulse was normalized to the value obtained during the initial test pulse. *P < 0.001. Fitting to a double-exponential function yielded the time constants as follows: τ_f = 9.32 ± 1.27 ms, τ_s= 30.95 ± 2.54 ms for WT (open circles, n = 55); τ_f = 17.27 ± 5.43 ms, τ_s = 32.26 ± 6.89 ms for G400A (filled circles, n = 8); P < 0.05 for difference in τ_f, but τ_s and fractional amplitudes were not significantly different as compared with WT.

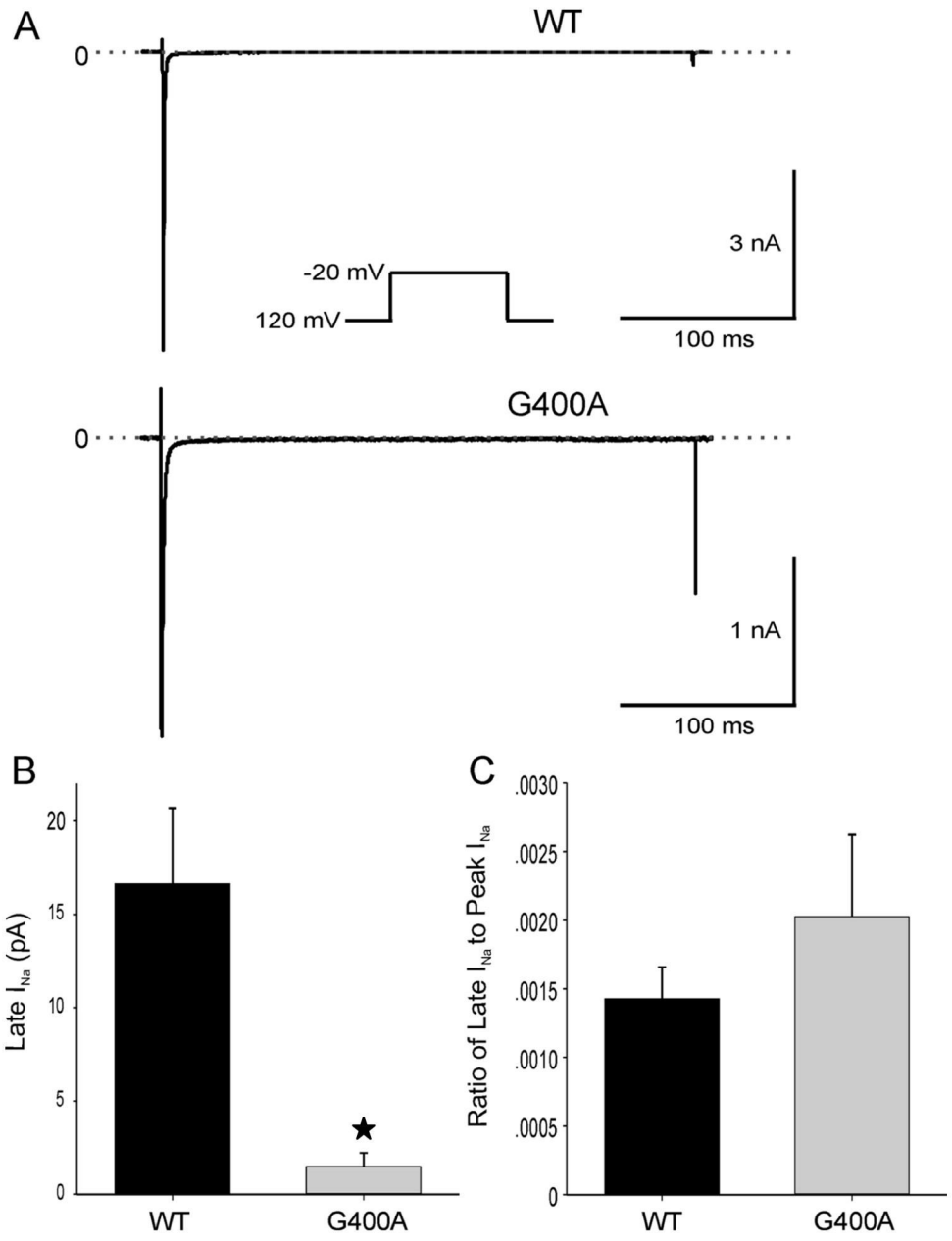

Figure 6.

Persistent inward sodium currents (late-I_{Na}) for WT and G400A. **A:** TTX-sensitive current obtained by subtraction. **B:** I_{Na} amplitude at the end of the 300-ms depolarization was 16.63 ± 4.06 pA (n=18) for WT channels and 1.48 ± 0.74 pA (n=6) for G400A mutant channels (*P < 0.05). **C:** I_{Na} amplitude at the end of the 300-ms depolarization was 0.14% ± 0.02% (n=18) of peak inward current for WT channels and 0.20% ± 0.06% (n=6) for G400A mutant channels (P > 0.05).

Table 1

Clinical Observations and Molecular Genetic Analysis of SCN5A in 19 AMI patients

Patient ID	Gender	Age	VT/ VF Episodes	MI Location	Culprit artery	Number of diseased coronary arteries	Site where VF occurred	SCN5A nonsynonymous Polymorphism	SCN5A mutation
MMRL23	M	70	6	Ant	LAD	1	ICU	H558R	G400A
MMRL48	M	50	1	Inf	RCA	2	E.R.	-	-
MMRL49	M	52	1	Inf	RCA	1	Cath Lab	-	-
MMRL51*	M	48	1	Inf	LCX	2	E.R.	-	-
MMRL52	M	43	1	Ant	LAD	1	OOH	-	-
MMRL53**	M	59	1	Inf	RCA	1	E.R.	-	-
MMRL54	M	53	2	Ant	LAD	1	Cath Lab	H558R	-
MMRL55*	M	52	1	Inf	RCA	1	OOH	H558R	-
MMRL56	M	58	2	Inf	RCA	1	OOH; Cath Lab	-	-
MMRL57	F	54	1	Ant	LAD	0[a]	OOH	-	-
MMRL58	M	63	1	Inf	LCX	1	E.R.	-	-
MMRL59	M	71	1	Inf	RCA	1[b]	ICCU	-	-
MMRL60	M	59	1	Inf	No	0[b]	H	H558R	-
MMRL61	M	66	1	Ant	LAD	1	E.R.	R34C	-
MMRL62	M	43	1	Inf	RCA	1	E.R.	-	-
MMRL63	M	46	1	Ant	LAD	2	OOH	-	-
MMRL64	M	54	1	Ant	LAD	1	E.R.	-	-
MMRL73	M	73	1	Ant	LAD	1	E.R.	H558R	-
MMRL74	M	77	1	Ant	LAD	3	E.R.	-	-

Laboratory; ICCU=Intensive coronary care unit; OOH = Out of hospital; H= Hospital ward other than ICCU.

Notes:

*Patients MMRL51 and 55 reported a history of familial sudden death. For patient MMRL53, this was his second inferior MI.

[a]Patients MMRL57 had irregular vessel with suspicious Myocardial infarction (MI) location: Ant=Anterior MI; Inf=Inferior MI; Site where the VF occurred: E.R.= emergency room

[b]Patients MMRL59 and 60 had Prinzemetal Angina.

Table 2

Gene Analysis of Potassium Channels in G400A Mutation Carrier

Gene	Nonsynonymous Polymorphism	mutation
KCNH2	-	-
KCNQ1	-	-
KCNE1	G38S*	-
KCNE2	-	-

G38S: heterozygous frequency 44.9%.

Dashes indicate negative results.